

Sequences of precipitate nucleation

K. C. RUSSELL

Department of Materials Science and Engineering, and Center for Materials Science and Engineering, Massachusetts Institute of Technology, Cambridge, Massachusetts, USA

H. I. AARONSON

Department of Metallurgical Engineering, Michigan Technological University, Houghton, Michigan, USA

Solid–solid nucleation theory, as recently extended to faceted nuclei, is applied to several problems in understanding experimentally observed sequences of precipitate nucleation involving transition phases during isothermal ageing. Transition precipitates form due to a low interfacial energy resulting from a greater structural similarity to the matrix than the equilibrium phase or succeeding transition phases and in spite of a usually smaller driving force, $|\Delta G_v|$, for nucleation than any of these competing phases. Transition phases formed after the first one are predicted to nucleate preferentially at the interphase boundaries of their predecessors, also on the basis of interfacial energy, rather than ΔG_v considerations. Most examples of precipitation sequences cited from the literature are in agreement with this prediction; the few exceptions found are noted and discussed. The preference of equilibrium phases for nucleating at high-energy grain boundaries and of transition precipitates for nucleation at dislocations and other lower energy sites is explained on the following basis. The high-energy boundaries reduce the net interfacial free energy needed for nucleation of either phase so much that the higher $|\Delta G_v|$ for the equilibrium phase becomes dominant. At the lower energy sites, the smaller reduction in ΔG^* , the free energy of activation for nucleation, provided makes the lower interfacial energy of the transition phases the dominant factor in causing such phases to nucleate more rapidly.

1. Introduction

The combination of the near ubiquity of transition phases in metallic alloy systems which can undergo precipitation from solid solution, the presence of a variety of nucleation sites and the preference of individual phases for specific types of site results in a considerable range of sequences of precipitate nucleation. Since these sequences are not only of much interest from the viewpoint of the mechanism of phase transformations *per se* but also control the evolution of the mechanical properties of precipitation-hardened alloys, a number of comprehensive efforts has been made to summarize and interpret the available experimental observations [1–6]. The present paper is of more restricted scope, focusing attention primarily on some new insights into particular

aspects of the overall theoretical problem which have developed out of recent [7] and current [8, 9] considerations of the influence of crystallography upon the mechanism and kinetics of solid–solid nucleation. Some of the concepts presented here have been previously proposed by others in less specific form; the availability of a more detailed formalism for the kinetics of nucleation will be seen, however, to permit more complete understanding of the specific effects of interest.

2. Solid–solid nucleation kinetics

The steady state rate of nucleation, J , is given by [10]:

$$J = Z\beta^*N \exp(-\Delta G^*/kT) \quad (1)$$

where Z = Zeldovich non-equilibrium factor

($Z \sim 10^{-2}$), β^* = rate at which solute atoms join the critical nucleus, N = number of atomic nucleation sites per unit volume, ΔG^* = free energy of activation for formation of the critical nucleus, and kT = the product of Boltzmann's constant and the absolute temperature.

The existence of particularly good lattice matching at certain orientations of the nucleus: matrix boundary is taken to result in the introduction of planar facets on the nucleus [7]. The nucleus morphologies considered are based upon one sphere for homogeneous nucleation and upon caps of two spheres for grain-boundary nucleation. In the particular examples treated, a facet is assumed, for simplicity, to be present at only one boundary orientation of a sphere or a spherical cap. Although faceting affects Z , β^* and ΔG^* in Equation 1, its predominant influence was found to be exerted upon ΔG^* , which in turn is the dominating factor in J [8].

Of the models treated [8], the two which are most useful in examining the present set of problems are the homogeneously nucleated faceted sphere (Fig. 1a) and the faceted grain-boundary allotriomorph (Fig. 1b and c). The precipitate phase is designated as β and the matrix as α . Application of the faceted sphere to nucleation at dislocations represents a quite crude approximation, but one which will be useful if it is kept in mind that the primary role of dislocations involves strain energy rather than interfacial energy [11–15]. The nuclei of Fig. 1b and c are appropriate for large-angle grain boundaries and coherent interphase boundaries, respectively.

For the faceted sphere of Fig. 1a [8]:

$$\Delta G^* = \frac{16\pi\sigma_{\alpha\beta}^3}{3(\Delta G_v + W)^2} (1 - 2f\{\alpha\}) \quad (2)$$

where $f\{\alpha\} = (2 - 3 \cos \alpha + \cos^3 \alpha)/4$, $\alpha = \cos^{-1}(\sigma_{\alpha\beta}^c/\sigma_{\alpha\beta})$, $\sigma_{\alpha\beta}$ = interfacial energy of a disordered (spherically curved) $\alpha:\beta$ boundary, $\sigma_{\alpha\beta}^c$ = interfacial energy of a partially or fully coherent facet, ΔG_v = volume free energy change attending nucleation and W = volume strain energy accompanying the formation of a critical nucleus. W should be zero for an incoherent nucleus [16] and can be calculated by the method of Eshelby [17], for the coherent case. Strain energies for partially coherent nuclei lie between these two extremes, but are very difficult to calculate. $f\{\alpha\}$, a common function in heterogeneous nucleation theory, is plotted versus α in Fig. 2. As $\sigma_{\alpha\beta}^c/\sigma_{\alpha\beta}$

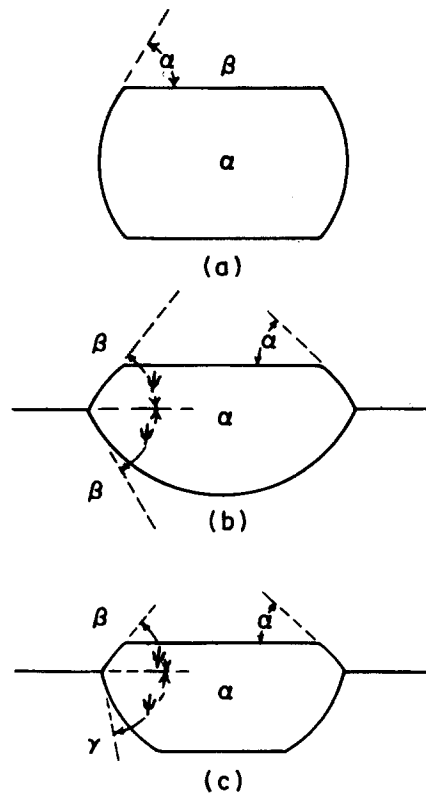


Figure 1 Possible faceted precipitate shapes for (a) homogeneous nucleation; (b) nucleation at a grain boundary; (c) nucleation at a coherent interphase boundary.

approaches zero (low energy facet), $\alpha \rightarrow \pi/2$, $f\{\alpha\} \rightarrow \frac{1}{2}$, $\Delta G^* \rightarrow 0$ and the nucleus becomes a disc of infinitesimal thickness. Clearly, an especially low value of $\sigma_{\alpha\beta}^c$ for one particular nucleating phase can result in the lowest possible ΔG^* in that system, assuming that $|\Delta G_v|$ is not too much

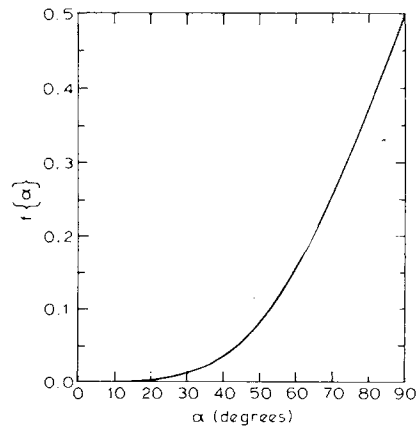


Figure 2 Dependence of catalytic potency function $f\{\alpha\}$ on contact angle, α .

smaller than for other possible phases. It should be noted, however, that excess vacancies can alter ΔG_v [16].

In the case of nucleation at a planar, disordered grain boundary of interfacial energy $\sigma_{\alpha\alpha}$ a facet may appear at one boundary orientation on only one side of the nucleus, as seen in Fig. 1b,† when no rational relationship exists between the nucleus and the adjacent matrix grain. For this nucleus,

$$\Delta G^* = \frac{16\pi\sigma_{\alpha\beta}^3}{3(\Delta G_v + W)^2} (2f\{\psi\} - f\{\alpha\}) \quad (3)$$

where the form of $f\{\psi\}$ is identical to that of $f\{\alpha\}$ and $\psi = \cos^{-1}(\sigma_{\alpha\alpha}/2\sigma_{\alpha\beta})$. ΔG^* thus decreases progressively through further truncation of the "upper" portion of the nucleus of Fig. 1b as $\sigma_{\alpha\beta}/\sigma_{\alpha\alpha}$ decreases from unity to $\sigma_{\alpha\alpha}/2\sigma_{\alpha\beta}$, where $\psi = \alpha$, and the facet becomes coincident with the grain boundary. ΔG^* continues to decline as $\sigma_{\alpha\beta}^c/\sigma_{\alpha\beta}$ is further reduced, becoming zero when $\sigma_{\alpha\alpha} = \sigma_{\alpha\beta} + \sigma_{\alpha\beta}^c$. Similar considerations apply to the model of Fig. 1c for nucleation at a coherent interphase boundary where facets may truncate both caps, at the same orientation when the two matrix phases are identical in crystal structure and orientation; details are given elsewhere [9].

Thus for both homogeneous and heterogeneous nucleation large reductions in ΔG^* , hence *exceedingly* large increases in the rate of nucleation may be effected by the inclusion of a facet (or facets) of sufficiently low energy in the interphase boundary of the critical nucleus. It is also qualitatively apparent, even though the quantitative details have yet to be developed, that further reductions in ΔG^* may be produced by the presence of facets at additional orientations of the nucleus: matrix boundary.

3. The nucleation sequence of transition phases

These ideas are conveniently expressed in terms of the transition phases in the prototypical Al-rich region of the Al-Cu system, but are of quite general applicability. They can be considered as a further development of the views of Hornbogen [5, 6] on this subject.

† ΔG^* for the nucleus of Fig. 1b is independent of the angle which the facet makes with the grain boundary as long as this angle is equal to or less than that needed to bring the facet into contact with the grain boundary. The quite difficult problem of ΔG^* for larger facet-boundary angles of this nucleus is considered elsewhere [18].

‡ Surprisingly, activity data do not appear to be available within this phase field.

3.1. From the viewpoint of volume free energy change

Fig. 3 shows the solvus temperatures for the equilibrium θ phase, the transitional θ'' and θ' phases and GP zones in Al-Cu. At ageing temperatures somewhat below all of these solvi, the precipitation sequence observed experimentally is [2, 19]:



Consideration of this precipitation sequence is begun upon the basis of the ΔG_v term in Equations 2 and 3. Assuming that the α Al-Cu solid solution is sufficiently dilute to allow replacement of activities‡ by compositions and that the precipitate phase is markedly solute-rich [20]:

$$\Delta G_v = \frac{RT}{V_\beta} \ln \frac{x_\alpha^{\alpha\beta}}{x_\alpha} \quad (4)$$

where R = gas constant, V_β = molar volume of the β (precipitate) phase, x_α = mole fraction solute, in the α matrix prior to ageing and $x_\alpha^{\alpha\beta}$ = mole fraction of solute in α at the $\alpha/(\alpha + \beta)$ solvus.

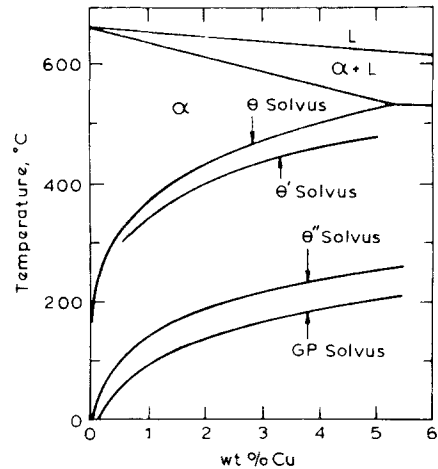


Figure 3 Solvi of θ , θ' , θ'' , and GP zones in the Al-Cu system. After Hornbogen [6] and Beton and Rollason [21].

It is important to note that during growth, the broad faces of GP zones and of θ'' plates remain fully coherent [2] and the broad faces of θ' plates become partially coherent quite slowly [22, 23].

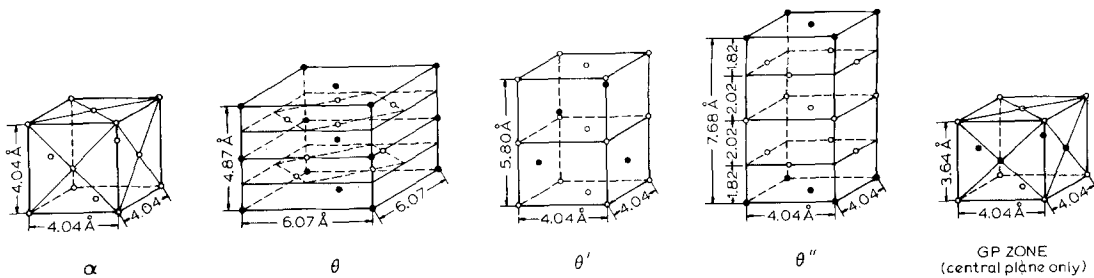


Figure 4 Crystal lattices of α , θ , θ' , and θ'' and GP zones in the Al-Cu system. After Hornbogen [6] and Gerold [24]. \circ , Al atoms; \bullet , Cu atoms.

Hence the solvus curves of these precipitates (see Fig. 3), even when properly determined by means of dissolution experiments, should represent the coherent solvi. Therefore, the volume strain energy associated with the broad face coherency is already accounted for and should not be algebraically added to ΔG_v . It thus follows from Fig. 3 that the nucleation driving force, ΔG_v , is successively more negative (at the same temperature and x_α) for GP zones, θ'' , θ' and θ ‡. If ΔG_v were the primary factor controlling the kinetics of nucleation, at a given temperature the θ phase would then be the first to nucleate, rather than the last. Hence another factor must be governing the sequence of precipitation; this factor will be seen to be that of interfacial energy.

3.2. From the viewpoint of interfacial energy

Fig. 4, from Hornbogen [6] and after Gerold [24], shows the lattices of the various precipitate phases in Al-4% Cu, and emphasizes their relationship to the fcc α Al-Cu matrix. The conjugate habit planes of the broad faces of θ'' and θ' are $\{100\}_\alpha$ in both matrix and precipitate phases [2]§. The edges of θ' plates are formed by a mixture of both $\{100\}_\alpha$ and $\{110\}_\alpha$ planes [27]. The small size, and especially the minute thickness and substantial coherency strains associated with GP zones and θ'' plates have prevented determination of the edge crystallography of these precipitates; probably with introduction of little error in the present considerations, θ'' plates will be

assumed to be bounded by $\{100\}_\alpha$ planes; in the case of GP zones, the details of edge crystallography are of little importance because these zones are simply monolayers of Cu [24]. The critical nuclei of these three phases may be reasonably assumed to have plate-shape morphologies qualitatively similar to those observed during the early stages of growth.

In considering σ , the specific interfacial free energy of an interphase boundary, the customary division is made into a structural component, σ_{str} (associated with interfacial misfit dislocations) [28] and a chemical component, σ_{chem} (resulting from a different proportion of the atoms of each species neighbouring atoms at the boundary viz viz those within each crystal). These components may be taken as additive [29].

The only component of σ to be considered for coherent GP zones is σ_{chem} . Using a relationship for this quantity due to Turnbull [29] and determining $\Delta \bar{H}^\circ$, the partial molar enthalpy of solution of Cu is an infinitely dilute solute of α Al-Cu, to be $4200 \text{ cal mol}^{-1}$ from the path of the GP zone solvus, for α :GP zone interfaces $\sigma_{\text{chem}} = 115 \text{ erg cm}^{-2}$.

Considering now the θ'' and θ' phases, the $4.04 \times 4.04 \text{ \AA}$ $\{100\}$ planes of each which match a plane of the same form and dimensions in the α lattice have a $\sigma_{\text{str}} = 0$. However, σ_{str} at the edges of plates of these phases may be seen from Fig. 4 to be appreciable in the case of θ'' and still larger in that of θ' . Both the θ'' and θ' lattices can be sectioned so that σ_{chem} , which is proportional to

‡ This is so if all phases have substantially the same composition. Otherwise, it is marginally possible that the order of driving forces for nucleation is different than the order of phase stabilities.

§ GP zones will be treated as homogeneously nucleated precipitates. Cahn [25] suggests that GP zones may be formed by spinodal decomposition, which would, of course, dominate any possible nucleation process. However, Lorimer [26] has demonstrated that the experimentally determined GP solvus matches the coherent solvus much better than the coherent spinodal in the Al-Zn system. Hence at least between these two calculated curves, GP zone formation in Al-Zn should be the product of homogeneous nucleation and growth. Insufficient information is available with which to calculate the coherent spinodal in Al-Cu and thus the possibility is not ruled out that GP zone formation in this system takes place by spinodal decomposition.

the square of the composition difference across the interphase boundary [29], is virtually zero across the broad faces of plates of these phases. σ_{chem} is substantial across the edges of θ'' plates, and still larger across those of θ' plates. It appears probable, in fact, that despite the relatively small proportion of the area of critical nuclei of θ'' and θ' which the edge orientation presumably occupies, σ_{str} for this orientation is sufficiently high so that the total $\sigma = \sigma_{\text{str}} + \sigma_{\text{chem}}$ for each transition phase increases in the order: GP zones, θ'' and θ' .

In the case of θ , while it is possible to form partially coherent facets with the α matrix [30], the overall level of matching between the α and θ lattices is seen from Fig. 4 to be sufficiently poor so that the average value of σ for $\alpha:\theta$ boundaries should be appreciably greater than that for the boundaries between α and the various transition precipitates.

In terms of the models for homogeneous and heterogeneous nucleation considered in the previous section, the foregoing considerations may be summarized by stating that when the effects of faceting are summed, the interfacial energy barrier decreases with progression through the series θ , θ' , θ'' and GP zones.† Once ΔG_v becomes sufficiently negative for all possible precipitates, the circumstance that ΔG^* is proportional to the product of some function of ψ and α and the third power of $\sigma_{\alpha\beta}$ but only to the negative second power of $\Delta G_v + W$ will tend to make the interfacial energy factor the dominant one, thus explaining the observed sequence of precipitates.

A more quantitative treatment of this problem requires determination of the equilibrium shape for each precipitate involved at the type of site at which it nucleates (this shape being a useful approximation of the critical nucleus shape). Kinetic factors, however, will make the necessary experimental determination of these shapes very difficult to accomplish.

4. Nucleation sites of successive transition phases

When the first transition phase to form makes its appearance, at least two depressant effects are exerted upon the nucleation probability of any

succeeding transition phases and of the equilibrium precipitate. First of all, ΔG_v for nucleation of the other phases becomes less negative at all nucleation sites lying within the (time dependent) diffusion fields of the individual precipitates of the first phase. Further, nucleation of the first transition phase consumes some proportion of the available nucleation sites, thereby reducing N in Equation 1. This may be a particularly important consideration if the initial phase forms on some easily saturable site, such as dislocations.

The extent of the diffusion field, and thus the reduction in $|\Delta G_v|$ for the nucleation of the remaining precipitate phases, is readily calculated for planar, spherical or cylindrical precipitates of the initial transition phase [32]. For typical numbers of precipitates per unit volume and ageing temperatures in Al-base alloys, the time required to produce overlapping of the diffusion fields of adjacent precipitates – a useful approximation of the time needed to make ΔG_v for further nucleation less negative essentially throughout the remaining volume of matrix – is of the order of seconds or minutes in quenched and aged alloys (where additional nucleation sites introduced during the quenching process expedite nucleation during subsequent ageing [33]) and somewhat longer if specimens are isothermally reacted immediately after solution annealing.

Given the foregoing handicaps which the nucleation and growth of the first transition precipitate impose upon the nucleation of subsequent precipitates, it is suggested that the nucleation of the next precipitate should occur preferentially at the interphase boundaries of the first one, and that succeeding precipitates ought to follow the same pattern. Supersaturation for the nucleation of β_{n+1} (the $(n+1)$ th phase to appear) is initially less at the interphase boundaries of phase β_n than at locations further removed from these boundaries. However, the greater importance of minimizing the interfacial free energy than of $|\Delta G_v|$ previously noted and the circumstances that interphase boundaries, being an areal type of defect, can usually contribute much more energy to the nucleation process than dislocations, should make the interphase boundaries of phase β_n the most favoured intragranular site for the nucleation

† Upon the basis of available experimental data on the relative σ 's of disordered interphase and grain boundaries [31], the assumption is made that energies of disordered boundaries between α and the various transition phases are unlikely to be much different. Hence $f\{\alpha\}$ should depend primarily upon $\sigma_{\alpha\beta}^0$. Also, $f\{\psi\}$ is taken to be similar for the equilibrium and for the various transition phases on the same grounds.

of phase β_{n+1} . The structural similarity often obtaining amongst successive transition phases should allow the formation, during the nucleation process, of $\beta_n:\beta_{n+1}$ boundaries of particularly low energy. Such boundaries are most useful in respect of reducing ΔG^* , however, when they replace $\alpha:\beta_n$ boundaries of relatively high interfacial energy.

Nucleation at locations other than interphase boundaries may be expected when the volume change accompanying the precipitation of β_n crystals is sufficiently large to cause extension of the original nucleation site into regions where ΔG_v is more negative, or the creation of new nucleation sites which also propagate into such regions. In the former category is included climb of the dislocation [34–38] on which nucleation initially occurred. Propagation of dislocations from the interphase boundary, for example by punching [39], is a good example of the second. Aggregation of vacancies resulting from accommodation of the volume change, when the average volume per atom is smaller in the precipitate than in the matrix, into small clusters some distance away from the interphase boundary is another possible example of the second type.

It is also possible, though none too probable, that the rate of nucleation of β_{n+1} is sufficiently similar to that of β_n so nucleation of β_{n+1} precipitates can occur at sensible rates either on the same type of defect as that favoured by β_n , or, more likely, on another type of defect, prior to the occurrence of a significant solute loss at such nucleation sites. The extreme sensitivity of the rate of nucleation to small differences in the variables comprising ΔG^* makes this type of exception difficult to accept unless the density of nucleation sites is quite high and the diffusivity in the matrix is low.

Evidence that one precipitate phase has nucleated at the interphase boundaries of another is best obtained by transmission electron microscopy. Acquisition of such evidence is not an uncommonly difficult task unless the particles of the first phase are very small and/or not easy to place in good contrast with respect to the matrix phase. These difficulties have complicated demonstration that precipitates nucleate at GP zones and in some cases extensive reliance has had to be placed upon indirect methods. Nonetheless, good evidence for this phenomenon has been obtained in a number of aluminium-base alloys [24,

40–45] and in some α Fe–X alloys [46–48]. Cases in which direct transmission electron microscopic evidence has been obtained for the nucleation of either another transition phase or the equilibrium phase at the interphase boundaries of a transition phase include the nucleation of θ at θ' in Al–Cu [49, 50], θ' at θ'' in Al–Cu [6], Fe_3C at $\text{Fe}_{2.4}\text{C}$ in α Fe–C [51], η (Ni₃Ti) at γ' in Ni–Cr–Ti [52], σ at α (or δ) in austenitic stainless steel [53, 54] and Cr_7C_3 at Fe_3C in steels containing less than 2% Cr [55].

However, there have also been some reports of independent nucleation of β_{n+1} . Such observations inevitably invite the question as to whether or not β_n precipitates were resolved at the operative nucleation sites prior to the observation of β_{n+1} , though the $\sim 50 \text{ \AA}$ resolution customarily achieved in routine practice at least partially vitiates this objection. However, good observations have made on nucleation of M_{23}C_6 apart from M_7C_3 in Fe–C–Cr and Fe–C–Cr–X [55, 56], of Fe_3C apart from $\text{Fe}_{2.4}\text{C}$ in Fe–C–Ni [57] and of V_4C_3 apart from Fe_3C in Fe–C–V [57] during the tempering of martensite. The density of nucleation sites for carbides is unusually high in these microstructures; the rate of carbon diffusion is also high but that of substitutional alloying elements is very low. At least during the nucleation of the alloy carbides, that portion of ΔG_v involving the alloying element may not have been much altered by the initial precipitate at an appreciable fraction of the available non-interphase boundary nucleation sites prior to the nucleation of the second precipitate. Partition of Ni between $\text{Fe}_{2.4}\text{C}$ and ferrite in the immediate vicinity of the $\alpha:\text{Fe}_{2.4}\text{C}$ boundaries, however, may have been involved in the failure of Fe_3C to form at $\text{Fe}_{2.4}\text{C}$ in Fe–C–Ni. On the other hand, occurrence of such precipitation in Fe–C also suggests the possibility that the addition of Ni may have significantly decreased the interfacial energy advantage of this mode of nucleation.

5. Preference of equilibrium precipitates for disordered grain boundaries and of transition precipitates for intragranular sites

5.1. At high-energy grain boundaries

These preferences are experimentally well established [1, 6]. For simplicity, consider the model of Fig. 1b to apply to the nucleation of both an equilibrium and a transition phase at a disordered

(high energy) grain boundary. Because $\sigma_{\alpha\alpha}$ has a relatively high value, ψ will be relatively small, as will $2f\{\psi\}$. A still further reduction in ΔG^* will be produced by $f\{\alpha\}$, and since $\sigma_{\alpha\beta}^c/\sigma_{\alpha\beta}$ should be lower for a transition than for an equilibrium phase, $2f\{\psi\} - f\{\alpha\}$ ought to also be smaller. However, the reduction in $f\{\psi\}$ is suggested to be sufficiently substantial for the equilibrium phase so that its larger $|\Delta G_v|$, as raised to the second power in Equation 3, will more than compensate for the smaller value of $2f\{\psi\} - f\{\alpha\}$. Thus, at a grain boundary, the equilibrium phase should have the smaller ΔG^* .

5.2. At dislocations

The effects of dislocations on nucleation have been considered by Cahn [12] and Gomez-Ramirez and Pound [11] for incoherent nuclei and by Larché [13], Lyubov and Solov'yev [14] and Dollins [15] for the coherent case. A detailed comparison between the effects exerted upon incoherent and coherent nuclei – which may be roughly equated to the equilibrium and to a transition phase, respectively – does not appear to have been made. However, inspection of the Cahn [12] and Gomez-Ramirez and Pound [11] treatments viz a viz that of Larché [13] suggests that the reduction in ΔG^* which can be achieved in the case of coherent nuclei is comparable to that obtained for incoherent nuclei. Combined with the smaller values of $\sigma_{\alpha\beta}^c$ characteristic of transition phases, this reduction is evidently sufficient to make ΔG^* consistently less for transition than for equilibrium phases at dislocations.

The strength of the influence which dislocations exert upon coherent nucleation may be most clearly apprehended from the work of Larché [13]. For spherical nuclei, the effect of elastic interaction with a nearby edge dislocation is to replace $\sigma_{\alpha\beta}$ in Equation 2 by

$$\sigma_{\alpha\beta} - \frac{\mu b (1 + \nu)}{9\pi (1 - \nu)} |\epsilon^T| \quad (5)$$

where b is the Burgers vector of the dislocation, μ is the shear modulus, ϵ^T is the stress-free transformation strain, and ν is Poisson's ratio. The other terms in Equation 2 (specifically, ΔG_v and W) are unchanged. For $b = 2.5 \times 10^{-8}$ cm, $\nu = 0.3$, $\mu = 4 \times 10^{11}$ erg cm $^{-3}$ and $\epsilon^T = 0.05$, the correction factor is a very significant 33 erg cm $^{-2}$. Nucleation may, however, be depressed near dislocations if the precipitate has little or no misfit

strain and has higher shear modulus than the matrix [13]. In this case the "hard" precipitate increases the strain energy associated with the dislocation.

Larché's calculations thus provide a physical basis for the observations of Hornbogen and Roth [58] that at small undercoolings coherent nucleation of γ' in Ni–Al–X alloys takes place preferentially at dislocations when the misfit between matrix and precipitate is appreciable, but not when alloying reduces the misfit effectively to zero.

6. Conclusion

Sequential precipitate nucleation has been discussed on the basis of straightforward solid–solid nucleation theory. It is noted that consideration of ΔG_v , the volume free energy change associated with nucleation, leads to a sequence of precipitation just the inverse of that experimentally observed in the prototypical Al-rich Al–Cu alloys. In agreement with Hornbogen [5, 6], the various transition phases and the equilibrium phases are concluded to nucleate in order of increasing precipitate:matrix interfacial energy.

The nucleation of β_{n+1} (the $(n + 1)$ th precipitate phase) is predicted to take place at the interphase boundaries of phase β_n on the grounds that partial depletion of the available ΔG_v by the formation of β_n (and any predecessors) makes imperative the large contribution of interfacial energy which β_n can offer to reducing ΔG^* to a level allowing detectable intragranular nucleation kinetics. A number of examples of precipitation sequences which fulfill this prediction is cited from the literature. Three exceptions, all involving the precipitation of carbides in tempered martensitic alloy steels, are also noted. These are ascribed to a combination of a high density of nucleation sites and the very slow diffusion of substitutional alloying elements in ferrite at the temperatures involved. Thus, nucleation of β_n did not alter the conditions for formation of succeeding phases, which precipitated independently, and at a slower rate.

The preference of equilibrium phases for nucleation at disordered grain boundaries and of transition phases for nucleation at intragranular sites is explained upon the basis of the large contribution to the interfacial free energy for nucleation which can be made by such grain boundaries. The smaller reduction in ΔG^* by the

lesser area of facets expected on an equilibrium precipitate is thus more than compensated for by the substantial contribution of grain-boundary energy. It then becomes possible for the larger $|\Delta G_v|$ from the equilibrium precipitate to make ΔG^* smaller for this phase than for a transition phase at disordered grain boundaries.

The theoretical studies of previous investigators [11–15] suggest that dislocations, especially those of edge type, are approximately as effective in reducing ΔG^* of transition (\approx coherent) as of equilibrium (\approx incoherent) precipitates. Taken in conjunction with the lower interfacial energies characteristic of transition precipitates, these are accordingly the phases most likely to be nucleated at dislocations. The work of Larché [13] shows, however, that this effect is important only when there is substantial misfit between the matrix and precipitate lattices. This prediction is consistent with the experimental observations of Hornbogen and Roth [58].

Acknowledgement

This investigation was supported by National Science Foundation Grants GH-37103 and GH-38558, for which grateful appreciation is expressed.

References

1. A. H. GEISLER, "Phase Transformations in Solids" (John Wiley, New York, 1951) p. 387.
2. A. KELLY and R. B. NICHOLSON, *Prog. Mat. Sci.* **10** (1963) 149.
3. R. B. NICHOLSON, "Phase Transformations" (Amer. Soc. Metals, Cleveland, Ohio, 1970) p. 269.
4. E. HORNBOGEN, "Precipitation from Iron-Base Alloys" (Gordon and Breach, New York, 1965) p. 1.
5. *Idem*, *Z. Metallk.* **56** (1965) 133.
6. *Idem*, *Aluminum* **43** (1967) 9.
7. H. I. AARONSON and H. B. AARON, *Met. Trans.* **3** (1972) 2743.
8. W. C. JOHNSON, C. L. WHITE, P. E. MARTH, P. K. RUF, S. M. TUOMINEN, K. D. WADE, K. C. RUSSELL and H. I. AARONSON, *Met. Trans.* **6A** (1975) 911.
9. P. E. MARTH, H. I. AARONSON, G. W. LORIMER, T. L. BARTEL and K. C. RUSSELL, in preparation.
10. K. C. RUSSELL, "Phase Transformations" (Amer. Soc. Metals, Cleveland, Ohio, 1970) p. 219.
11. R. GOMEZ-RAMIREZ and G. M. POUND, *Met. Trans.* **4** (1973) 1563.
12. J. W. CAHN, *Acta Met.* **5** (1957) 169.
13. F. LARCHÉ, in "Dislocations", edited by F. R. N. Nabarro, in press.
14. B. YA. LYUBOV and V. A. SOLOV'YEV, *Fiz. Met. Metallov.* **19** (1965) 333.
15. C. C. DOLLINS, *Acta Met.* **18** (1970) 1209.

16. K. C. RUSSELL, *Scripta Met.* **3** (1969) 313.
17. J. D. ESHELBY, *Proc. Roy. Soc.* **A241** (1957) 376.
18. J. K. LEE and H. I. AARONSON, *Acta Met.*, in press.
19. H. K. HARDY and T. J. HEAL, *Prog. Met. Phys.* **5** (1954) 143.
20. H. I. AARONSON, K. R. KINSMAN and K. C. RUSSELL, *Scripta Met.* **4** (1970) 101.
21. R. H. BETON and E. C. ROLLASON, *J. Inst. Metals* **86** (1958–59) 77.
22. G. C. WEATHERLY and R. B. NICHOLSON, *Phil. Mag.* **17** (1968) 801.
23. R. SANKARAN and C. LAIRD, *ibid* **29** (1974) 179.
24. V. GEROLD, *Z. Metallk.* **45** (1954) 593, 599.
25. J. W. CAHN, *Trans. Met. Soc. AIME* **242** (1968) 166.
26. G. W. LORIMER, *Fizika* **2** Suppl. 2 (1970) 33.1.
27. C. LAIRD and H. I. AARONSON, *Trans. Met. Soc. AIME* **242** (1968) 1393.
28. J. H. VAN DER MERWE, *J. Appl. Phys.* **34** (1963) 117, 123.
29. D. TURNBULL, "Impurities and Imperfections" (Amer. Soc. Metals, Metals Park, Ohio, 1955) p. 121.
30. K. R. KINSMAN, H. I. AARONSON and C. LAIRD, *Acta Met.* **15** (1967) 1244.
31. C. S. SMITH, "Imperfections in Nearly Perfect Crystals" (John Wiley, New York, 1952) p. 377.
32. C. ZENER, *J. Appl. Phys.* **20** (1949) 950.
33. H. I. AARONSON and C. LAIRD, *Trans. Met. Soc. AIME* **242** (1968) 1437.
34. J. D. EMBURY, Ph.D. Thesis, Cambridge University (1963) see [3].
35. J. S. T. VAN ASWEGEN and R. W. K. HONEYCOMBE, *Acta Met.* **10** (1962) 262.
36. J. M. SILCOCK, *J.J.S.J.* **201** (1963) 409.
37. F. B. PICKERING, "The Relation Between the Structure and the Mechanical Properties of Metals" (H.M.S.O., London, 1963) p. 397.
38. J. M. SILCOCK and W. T. TUNSTALL, *Phil. Mag.* **10** (1964) 361.
39. G. C. WEATHERLY, *ibid* **17** (1968) 791.
40. M. SIMERSKA and VY. SYNECEK, *Acta Met.* **15** (1967) 223.
41. M. H. JACOBS and D. W. PASHLEY, "The Mechanism of Phase Transformations in Crystalline Solids, (Institute of Metals, London, 1969) p. 43.
42. G. W. LORIMER and R. B. NICHOLSON, *ibid* p. 36.
43. *Idem*, *Acta Met.* **14** (1966) 1009.
44. H. A. HOLL, *Met. Sci. J.* **1** (1967) 111.
45. D. W. PASHLEY, M. H. JACOBS and J. T. VIETZ, *Phil. Mag.* **16** (1967) 51.
46. E. HORNBOGEN, *Acta Met.* **10** (1962) 525.
47. *Idem*, *ibid* **10** (1962) 1187.
48. *Idem*, *Trans. ASM* **57** (1964) 120.
49. M. NEMOTO and S. KODA, *Nippon Kinzoku Gakkai-si* **27** (1963) 599.
50. C. LAIRD and H. I. AARONSON, *Acta Met.* **14** (1966) 171.
51. E. SMITH, "Direct Observation of Imperfections in Crystals" (Interscience, New York, 1962) p. 203.
52. H. F. MERRICK and R. B. NICHOLSON, "Proceedings Fifth International Conference on Electron Microscopy", paper K.8 (Academic Press, New York, 1962).

53. F. B. PICKERING, "Precipitation Processes in Steel" (Iron and Steel Inst. Spec. Rep. 64, 1959) p. 118.
54. L. I. SINGHAL and J. W. MARTIN, *Acta Met.* **16** (1968) 1441.
55. E. TEKIN and P. M. KELLY, *J.I.S.I.* **203** (1965) 715.
56. J. BEECH and D. H. WARRINGTON, *ibid* **204** (1966) 460.
57. E. TEKIN and P. M. KELLY, "Precipitation from Iron-Base Alloys" (Gordon and Breach, New York, 1965) p. 173.
58. E. HORNBOGEN and M. ROTH, *Z. Metallk.* **58** (1967) 842.

Received 24 February and accepted 20 March 1975.